Jordanian Journal of Computers and Information Technology (JJCIT), Vol. 08, No. 02, June 2022.

NEUROMORPHIC COMPUTING BASED ON STOCHASTIC SPIKING RESERVOIR FOR HEARTBEAT CLASSIFICATION

Chia Yee Saw[1] and Yan Chiew Wong[2]

(Received: 19-Jan.-2022, Revised: 18-Mar.-2022, Accepted: 6-Apr.-2022)

ABSTRACT

Heart disease is the leading cause of mortality worldwide. The precise heartbeat classification usually requires a higher number of extracted features and heartbeats of the same class may also behave differently in patients. This will lead to computation overhead and challenges in hardware implementation due to the large number of nodes utilized in reservoir computing (RC) networks. In this work, a reservoir computing-based stochastic spiking neural network (SSNN) has been proposed for heartbeat rhythm classification, enabling a patient adaptable and more efficient hardware implementation with low computation overhead caused by minimum extracted features. Only a single feature is employed in template matching to achieve patient adaptability with minimal computation overhead. The single feature, QRS complexes, was extracted and fed into the neural reservoir with 20 neurons in a cyclic topology for arrhythmia similarity calculation and classification. 43 recordings of Electrocardiogram (ECG) signals that included both normal and arrhythmic beats from MIT-BIH arrhythmia database obtained from Physio-Net were used in this work. The proposed stochastic spiking reservoir achieves a sensitivity of 99.6% and an accuracy of 96.91%, signifying that the system is accurate and efficient in classifying normal and abnormal arrhythmias.

KEYWORDS

Neuromorphic computing, Stochastic, Reservoir, Spiking neural network, Template matching, Arrhythmia, ECG classification

1. INTRODUCTION

According to the Centers for Disease Control and Prevention (CDC), heart disease caused the deaths of approximately 659,000 people in the United States each year [1]. The United States spent $363 billion on heart disease per year between 2016 and 2017. This comprises the expenditures of medical services and medications, as well as lost productivity as a result of mortality.

ECG signals are a useful instrument that has been widely employed in numerous applications for the investigation of cardiac diseases [2]–[4]. ECGs use electrodes to monitor the electric activity generated by the flexion and contraction of heart muscles [5]. The ECG results show the physical activity of the heart, indicating whether the heart is healthy or has an abnormal rhythm. Abnormal rhythm is often known as arrhythmia, which is the most common cause of cardiac illness.

In recent years, various computer-assisted diagnostic approaches for classifying heartbeats for arrhythmia prediction have been proposed. To achieve automated real-time classification approaches, lower computational cost and easy adaptability to hardware are necessary [6]-[8]. Neuromorphic computing is a potential alternative to conventional von Neumann computers for specialized sensory-processing or classification applications. Neuromorphic systems imitate the biophysics of neuro-biological networks by imitating the information processing mechanism of biological neurons and synapses [9]. Through repeating this basic cortical columnar arrangement of neurons and synapses, a biological brain discovers a cognitive computing pattern that is highly energy-efficient. Neuromorphic architectures are known for their ability to perform complex machine-learning tasks with high connectivity and parallelism on a smaller footprint more than conventional von Neumann systems [10]–[13]. These characteristics contribute to the implementation of neuromorphic architectures in hardware development.

However, a high number of features in ECG recognition leads to excessive hardware calculation

C. Y. Saw and Y. C. Wong are with Faculty of Electronic and Computer Engineering (FKEKK), Universiti Teknikal Malaysia Melaka (UTeM), Malaysia. Email: ycwong@utem.edu.my

overhead that most of the previous research works have paid less consideration to. C. Venkatesan proposed a k-Nearest Neighbours-based (kNN) arrhythmic beat classification approach that classified normal and abnormal ECG signals utilizing 14 time domain and frequency domain heart rate variability (HRV) features with an accuracy of 97.5 % [14]. In another study, Ye et al. employed multiclass classification with Support Vector Machine (SVM) with 5 features comprising morphological, wavelet, RR interval, independent component analysis (ICA) and principal component analysis (PCA) to differentiate between normal and abnormal signals [15]. Vedavathi et al. used the kNN algorithm to classify abnormal beats based on three features: higher-order statistics (HOS), spectral characteristics and temporal features [16]. S. Savalia et al. used deep neural network approaches, such as multi-layer perceptron (MLP) and convolution neural network (CNN) with three characteristics: P wave, QRS complex wave and T wave for arrhythmia classification [17]. S. Nahak suggested a fusion-based SVM for arrhythmia classification, which achieved a three-class classification accuracy of 93.33% [18]. Thus, in this work, template matching technique has been proposed using minimum feature extraction from the ECG signal while still maintaining accuracy in order to reduce the computational burden of the system, achieving efficient hardware implementation.

In terms of adaptability to hardware, field programable gate array (FPGA) is a potential hardware solution for this application, where a large portion of the electrical functionality inside the device can be customized with low implementation cost [19]-[21]. Mariel et al. proposed a parallel continuous neural network (CoNN) using FPGA for arrhythmia detection [19]. The categorization algorithms in prior study utilized characteristics including amplitude, phase and signal shape. The identifier is implemented using a total of 50284 lookup tables (LUT) and 471 flip-flops (FF). An FPGA-based back propagation neural network (BPNN) implementation was proposed by Egila et al. to categorize ECG signals [20]. The developed module employs Discrete Wavelet Transform (DWT) for feature extraction to extract four features while using significantly less hardware. W. Matthias et al. presented multiple MLP-based ECG anomaly detection implemented in Zynq FPGA; however, it still requires a lot of hardware resources. For instance, the proposed 10-6-2 12-bit multilayer perceptron requires 1613 FF and 1963 LUTs [21]. Although BPNN and MLP require significantly lower hardware resources, there are still difficulties in dealing with inter-patient variability. However, it must be noted that the hardware implementation of neural network suffers from resource constraints because of the typically large number of nodes utilized in RC networks and the high chip area required by the activities engaged with each processing node [22]. The proposed stochastic computing (SC) approach and simple cycle reservoir (SCR) architecture implemented in SSNN significantly minimized the number of connections, resulting in a more efficient hardware implementation.

Inter-patient variability is a crucial concern in ECG data, since heartbeats of the same class can behave differently in patients. Template matching approach was implemented to overcome the concern of inter-patient variability. Most of the research in the literature focused on simple arrhythmia classification, which categorizes arrhythmia based on distinct features without patient adaptability feature. In this work, we propose a high-performance arrhythmia detection system that uses stochastic spiking RC to have a minimal processing overhead and minimize inter-patient variability concerns. In contrast to other research in the literature, a high performance for arrhythmia classification is achieved by utilizing only one feature, the QRS complex.

Section 1 presents an extensive assessment of recent studies on arrhythmia classification, while Section 2 presents literature on spiking reservoir learning machine and architecture. Section 3 presents the proposed ventricular heartbeat classifier, including Pan Tompkins beat detection algorithm, feature extraction and stochastic neuron design. Section 4 presents the performances of R-peak detection and arrhythmia classification. Hardware resource utilization and feature size of the proposed classifier are then compared with those of previous studies. The conclusion is made in Section 5.

2. SPIKING RESERVOIR LEARNING MACHINE

Spiking reservoir network is a class of brain-inspired recurrent algorithms known as RC networks, aiming to reduce computational complexity and cost of training machine-learning models by using random, fixed synaptic strengths. In this work, the RC network has been built using a three-layer spiking neural network (SNN) to compute spikes encoded, a dynamic system and a readout mechanism and with little effort, it can achieve machine-learning functionality.

2.1 Spiking Neural Network (SNN)

Spiking neural networks are the most recent generation of Artificial Neural Networks (ANNs), in which neuron models communicate by sequences of spikes to process large amounts of data [14]-[15]. The information is encoded in the rate and timing of the spikes' arrival.

Figure 1shows two connected biological neurons which communicate through sequences of spikes. The incoming signals from connected neurons accumulated by dendrites are spatially and temporally summed by the cell's body. The neuron will generate a spike if it receives enough input that exceeds the threshold. The action potential is transmitted along the axon to other neurons of the nervous system. If the threshold is not surpassed, this indicates that insufficient input was received; the inputs fade quickly and no action potential is produced.

The conventional artificial sigmoidal neuron is used to model the spiking neuron, which uses firing rate to relay neural information. The sigmoidal unit's operation is depicted in Figure 2. A weight variable describing the strength of the influence on the postsynaptic neuron is used to simulate the synapse between two neurons. Positive and negative weights are used to represent excitatory and inhibitory synapses, respectively. The potential of a sigmoidal neuron is calculated by adding together all of the weighted firing rates of its presynaptic neurons. The activation function is used to determine the neuron's output from this potential which has a sigmoid form.

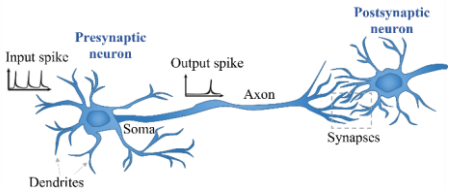

Figure 1. Biological neurons.

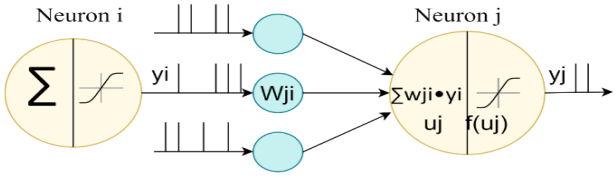

Figure 2. Basic operation of sigmoid neuron.

2.2 Reservoir Computing (RC)

RC is a computational architecture developed by recurrent neural network theory that maps input signals into higher-dimensional computational spaces utilizing the dynamics of a reservoir, which is a fixed, non-linear system. The reservoir is expected to be sophisticated enough to collect a significant number of input stream properties that can be utilized by the reservoir-to-output readout mapping [23].

Contrary to conventional Recurrent Neural Networks (RNNs) that need to adjust all connections to minimize the training error, the key characteristic of RC is that only the readout weights W_{out} are trained with a basic learning method such as linear regression, whereas the input weights W_{in} and recurrent connection weights W inside the reservoir are not trained [16], [18]. General RNN architecture and RC system are illustrated in Figure 3. This strategic design simplifies the complicated and time-consuming training procedure of traditional fully trained RNNs to a simple linear regression issue, which is greatly simplifying RNN implementation [19]-[20].

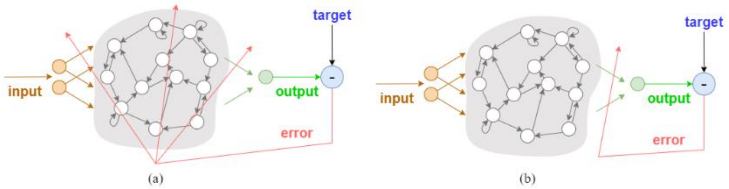

Figure 3. (a) General RNN architecture (b) RC system.

3. Proposed Ventricular Heartbeat Classifier

Figure 4 depicts the procedures of the proposed technique. Signal denoising minimizes baseline drift and power-line interference that are typically emphasized in ECG signals. The peak detection detects the R-peak location and amplitude. The samples around each R-peak location are retrieved in a window by QRS segmentation. QRS complex is then employed in the spiking neural network for machine learning and classification. The correlation coefficient calculated from template matching was used to analyze the similarity between typical normal beats and the test beat. In this project, the well-known Pan

Tompkins beat detection algorithm is applied. This algorithm used band-pass filtering, signal differentiation, squaring, moving window integration and two sets of adaptive thresholds to filter and integrate signals for beat detection [24].

3.1 Signal Denoising

There are a variety of sounds and anomalies in polluted signals, but baseline drift and power-line interference [26] are two types of noise that are often highlighted in ECG signals. The impression of baseline wander (BW) occurs when a signal's base axis appears to "drift" up and down, causing the entire signal to deviate from its baseline. Baseline wander is a low-frequency distortion in the ECG caused by electrically charged electrodes, patient movement and respiration [27]. Power-line interference is another common cause of noise which must be removed from the signals, because it fully obliterates the low frequency P and T waves in ECG signals. These noises and artifacts can impede the extraction of useful information from the raw ECG signal, resulting in an incorrect diagnosis and having a significant impact on the performance of algorithms during classification [23], [28]-[29].

The initial step was to use band-pass filtering composed of a cascaded high-pass and low-pass filters with a passband of 5-15 Hz, to remove BW and 50 Hz power- line interference and reduce the T wave amplitude. Figure 5 shows the ECG signal pre-processing process.

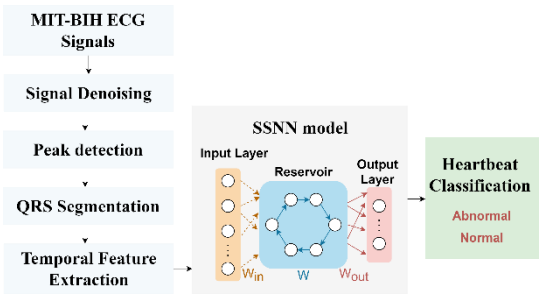

Figure 4. Schematic representation of ventricular heartbeat classifier [25].

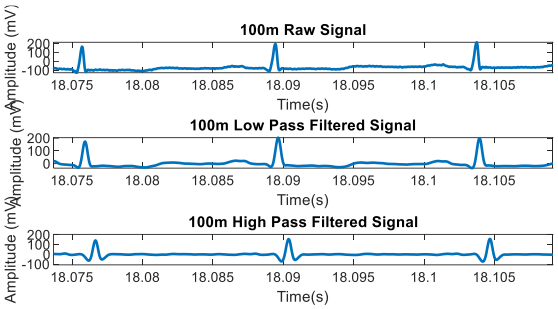

Figure 5. ECG signal denoising.

3.2 Peak Detection

The signal was differentiated after the band-pass filtering stage to highlight the severe slopes of the QRS complex. The squaring operation increases the slope of the derivative's frequency response curve to extract the R-peaks. The moving window integrator generates a signal including slope and QRS complex width information. The locations and amplitudes of R-peaks in the ECG signal were detected and stored in $R^{n\times m}$ matrix in a row-wise format, where n = 2 consists of location and amplitude of the R-peak and m is the number of detected R-peaks. Figure 6 shows an example of applying the Pan Tompkins algorithm for R-peak detection in the MIT-BIH arrhythmia database.

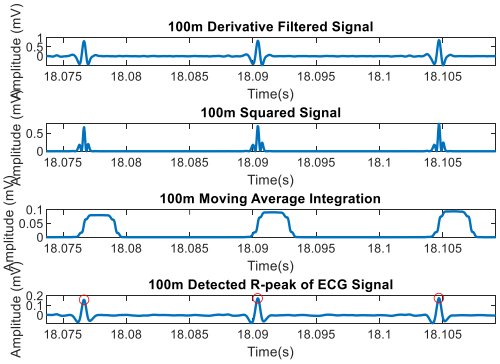

Figure 6. ECG signal peak detection.

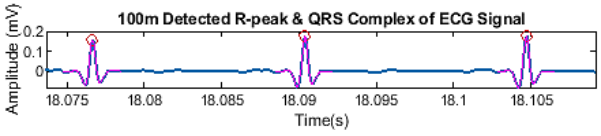

Figure 7. QRS segmented area in the ECG signal.

3.3 QRS Segmentation

The R-peak location contained in the $R^{n\times m}$ matrix is chosen as a reference point. After determining the R-peak location, 75 samples around each R-peak were extracted in the window and counted as a single

heartbeat. The window only spans the duration of the QRS complex rather than the whole cardiac cycle. Figure 7 depicts the segmented region based on the QRS complex. The Q wave and S wave reflect the beginning and end point of the highlighted beat, whereas the R wave represents the peak area. The heart's ventricular depolarization is represented by the combination of Q, R and S waves [30].

3.4 Temporal Feature Extraction

The main interest of this research is to extract representative features with minimal calculation overhead and avoid inter-patient variability concerns. The simple and patient-adaptive technique template matching is utilized to alleviate the inter-patient variability difficulties outlined in Section 1. This approach is utilized to determine the similarity between the signal beat and the same class-specific template, then employed a normalized correlation coefficient defined as an equation to classify the data as shown in Figure 8.

$$\gamma_{xy}(k) = \frac{\sum_{n=0}^{N-1}[x(n)-\bar{x}][y(n-k)-\bar{y}]}{\sqrt{\sum_{n=0}^{N-1}[X(n)-\bar{x}]^2 \sum_{n=0}^{N-1}[y(n-k)-\bar{y}]^2}} \quad (1)$$

where γ_{xy} represents the correlation coefficient, N represents the number of template points, x(n) represents the template points, y(n) represents the signal points under investigation, $\bar{x}$ represents the average of the template points and $\bar{y}$ represents the average of the signal points and k represents the time index of the signal y(n) at which the template is placed. The correlation coefficient is in the range $-1 < \gamma_{xy} < +1$, where +1 means that the signal and template are perfectly matched.

Template matching approach is implemented in this work with a lower computation complexity while retaining a high compression ratio and a minimal reconstruction error. This study excludes from consideration those signals for the feature extraction phase that have contamination in their sections.

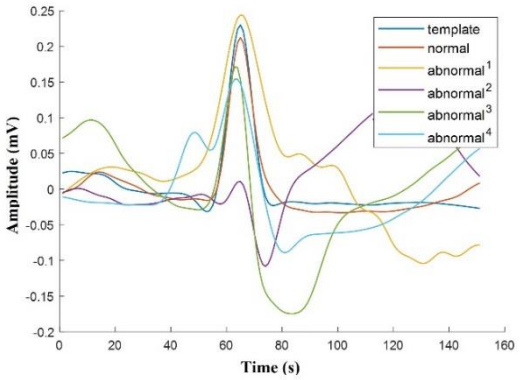

Figure 8. Template matching of segmented heartbeat.

The classification of normal and abnormal heartbeats is proposed by medical specialists in previous research [31]-[32]. Normal heartbeats have regular RR intervals, with the existence of a P-wave and a narrow QRS complex, whereas abnormal heartbeats have a shorter RR interval, no P-wave and a broader QRS complex.

3.5 Stochastic Spiking Neural Network

SSNNs are a recently proposed hardware solution based on a simple spiking neuron model capable of reproducing the probabilistic nature of synaptic transmissions, thus replicating the intrinsic stochastic behaviour of real biological neurons. The main distinction between SNNs and other neural networks is that SNNs explicitly model time. The concept is that neurons in the SNN do not communicate information at the end of each propagation cycle, but rather only when a membrane potential exceeds the threshold.

The retrieved QRS complex in the preceding section was employed as an input signal for the neural reservoir with 20 neurons. The stochastic neuron system contains three fundamental stages, as shown in Figure 9, binary to pulse conversion, SC and pulse to binary conversion. The input from the feature extraction process is converted into a binary number in the SSNN process by using analog-to-digital converter which transforms the analog input signal into the binary output signal. The binary value data

is first transformed into a pulse signal for stochastic computation and then the pulse signal is converted into its equivalent binary value again.

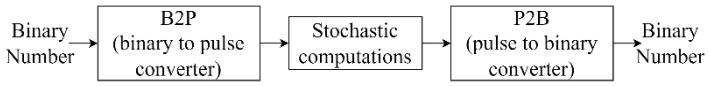

Figure 9. Stochastic computing system's fundamental stages.

3.5.1 Stochastic Computing (SC)

SC is a paradigm that counts the number of ones in a bitstream called a stochastic number, which is expressed as a fraction p=n/N, where n is the number of 1s in binary sequences and N is the length of binary sequences. For instance, the bitstream 01000010 contains two ones in an eight-bit stream, corresponding to a represented number of p=P(X=1) = 2/8 = 0.25. Figure 10 depicts the basic SC circuits, where the real number x is represented in unipolar format (UP) in the range [0, 1] and bipolar format (BP) in the range [-1, 1].

SC is utilized in this research by implementing digital gates in the SSNN. The proposed method reduces the amount of hardware required to perform arithmetic operations by employing probabilistic computing concepts. The multiplication in multiple-accumulate (MAC) operation could be easily realized by using a two-input XNOR gate for the bipolar coding format, as shown in Figure 10(b), followed by the scaled addition operation with a multiplexer (MUX), as shown in Figure 10(d).

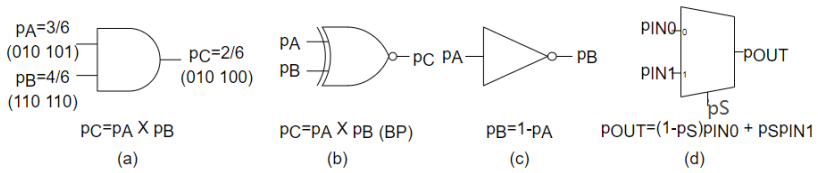

Figure 10. Basic circuits used in stochastic computation (a)AND (b)XNOR (c)NOT (d)MUX.

3.5.2 Binary-to-Pulse Converter (B2P)

The conversion from binary magnitudes (X) to pulsed stochastic signals (x) is performed by the B2P block shown in Figure 11. A random number generator (RNG) is used to create a pseudo-random binary number in each clock cycle, which is then compared to the n-bit input binary number with evaluation period T_{eval}. The comparator is actively high when $X > R_N$; otherwise it is maintained low. The comparator's output results in a bitstream $x = X/2^n$ with probability of getting 1.

3.5.3 Pulse-to-Binary Converter (P2B)

The P2B block is shown in Figure 11. Figure 12 is used to complete the process of converting the pulse signal x into its equivalent binary value X. It consists of two n-bit counters and an n-bit register. The first counter counts the number of high values (1s) given by the stochastic signal throughout the N_c clock cycle. The second counter is used to reset the first counter and load a new value for the register every N_c clock cycle. Therefore, the P2B block generates an n-bit number that changes per N_c cycle.

The block's output is a binary number that will remain stored for N_c =2n-1 clock cycles until being updated with the next integration value. However, this conversion incorporates a statistical error. Thus, linear feedback shift register (LFSR) was implemented in this project and extended bit sequences were analyzed to obtain correct results. The probability of receiving an output corresponding to high-level values in a series of the random variable p(t) over Nc clock cycles is calculated using the binomial distribution equation:

$$Prob(X) = \binom{Nc}{X} p^X (1-p)^{Nc-X} \quad (2)$$

3.6 Stochastic Neuron Design

The proposed stochastic neuron design consists of a few simple digital blocks: logic gates, a multiplexer, an LFSR, a register and a comparator. Figure 13 shows a single two-input sigmoid SC-based neuron with n=8 and evaluation time to $N_c=2^8$-1 clock cycles.

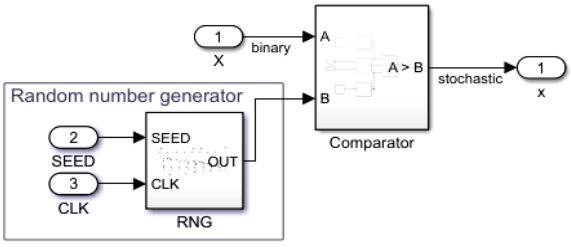

Figure 11. B2P converter block.

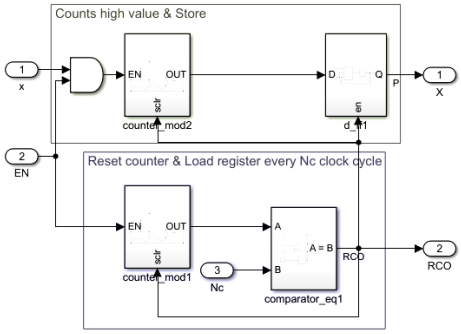

Figure 12. P2B converter block.

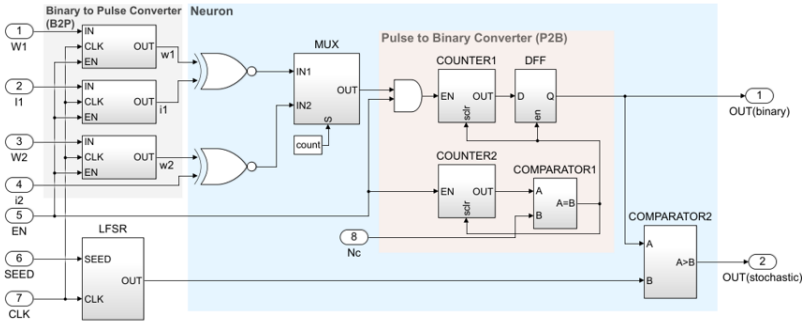

Figure 13. Two-input SC-based sigmoid neuron.

The input and weight binary values are first converted into pulsed signals using B2P converter before being processed by the stochastic circuit. The first input signal I_1 is a binary magnitude that is externally supplied to the system, but the second input signal i_2 is a stochastic bitstream that receives directly from another neuron. An XNOR gate and a multiplexer are used in the stochastic computing architecture to perform multiplication and addition operations. The resultant bitstream from the input weighting and addition is converted into a binary integer through P2B converter. The binary result is transformed back into a stochastic bitstream for further processing by another neuron.

20 stochastic neurons that make up the SSNN have been arranged based on SCR architecture as shown in Figure 14. This topology decreased the number of connections and simplified the automated network design, allowing for more efficient hardware implementation, when compared to previous research that employed random connections.

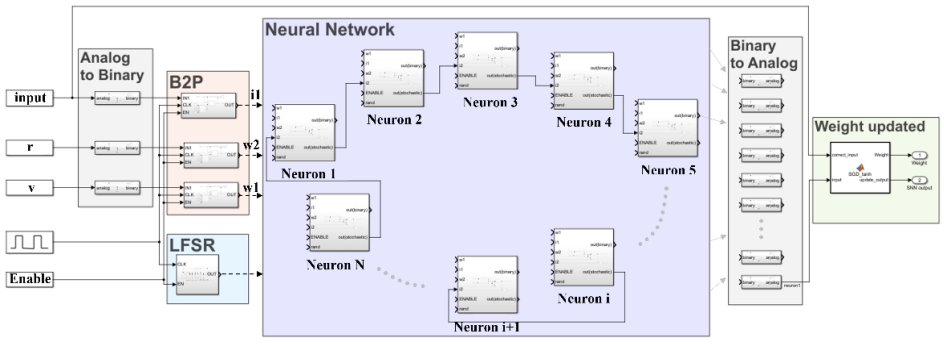

Figure 14. SSNN composed of 20 stochastic neurons in cyclic topology.

3.7 SNN Activity

The SNN's activity is depicted in Figure 15. The input spikes entering the counter appear to contribute to an increase in the membrane over-voltage. During the evaluation process, the incoming pulses are added up per clock cycle T_{clk} in the counter, where the evaluation period is basically a definite number of clock cycles: $T_{eval} = N_c \cdot T_{clk}$. A random number generator is used to produce the value of the variable threshold V_k. The value of the estimated over-voltage corresponding to the preceding evaluation period is compared to the reference voltage per clock cycle. If membrane over-voltage S_k exceeds V_k, the

neuron emits a spike X_k =1; otherwise it remains at a low level X_k =0.

Figure 16 depicts QRS complex as the input signal associated with the output of various nodes in the reservoir. Each neuron state oscillates in response to the input stimuli and this information is utilised to calculate the network's prediction output. It can be observed that a good match occurs as the number of neurons trained increases.

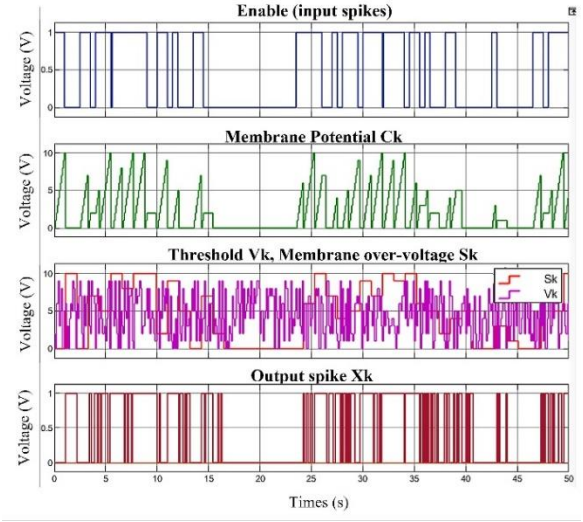

Figure 15. Temporal evolution of the different signals in the SNN model.

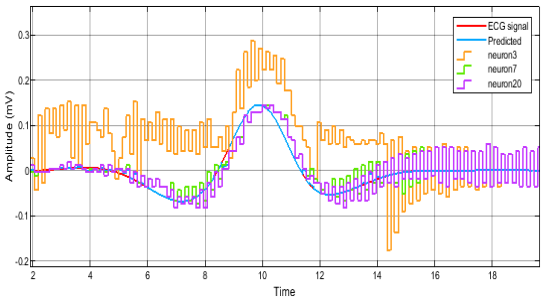

Figure 16. Three chosen neurons' output from the reservoir along with QRS complex input signal.

4. Results, Analysis and Discussion

The classification was carried out using the MIT-BIH arrhythmia database, which includes 43 recordings of ECG signals that included both normal and arrhythmic beats, each with a 30-min duration and a sampling rate of 360 Hz.

4.1 Performance of R-peak Detection

The Pan-Tompkins algorithm is used for R-peak detection and QRS segmentation. The performance of R-peak detection was evaluated using the following metrics: sensitivity (SEN), positive predictive value (PPV) and cumulative statistical index (CSI) and detection error rate (F_d) which are described in detail as follows:

$$SEN = \frac{TP}{TP+FN} \times 100 \quad (3)$$

$$PPV = \frac{TP}{TP+FP} \times 100 \quad (4)$$

$$CSI = \frac{1}{2}(SEN + PPV - FPR - FNR) \times 100 \quad (5)$$

$$F_d = \frac{FP+FN}{TP+FN+FP} \quad (6)$$

Table 1 reveals the overall performance of the R-peak detection on the MIT-BIH database, where out of a total of 97,963 beats, 205 and 227 beats were recognized as FP and FN, respectively. In addition, the proposed approach attained a minimum detection error of 0.44% with SEN, PPV and CSI at 99.8%, 99.8% and 99.6%, respectively. As a result, the Pan-Tompkins algorithm has an outstanding detection with minimal error detection, with high PPV indicating that a high proportion of R-peaks in the test beats are correctly detected, where high sensitivity indicates that the proposed approach is patient-adaptive and capable of detecting small outbreaks that behave differently in patients and larger CSI values indicate better overall detection performance.

Table 1. Evaluation results of R-peak detection.

	TP	FP	FN	SEN (%)	PPV (%)	CSI (%)	F_d (%)
Total	97963	205	227	99.8	99.8	99.6	0.44

True positive (TP) indicates a correctly detected R-peak, false negative (FN) indicates a missing R-peak and false positive (FP) indicates an incorrectly identified R-peak. False positive rate is FPR = FP/(FP+TP) and false negative rate is FNR = FN/(FN+TP). F_d was employed to calculate the detection error rate. Better detection performance is predicted by higher SEN, PPV and CSI values, while a lower F_d is expected. In Table 1, the TP, FP, FN, SEN, PPV, CSI and F_d values of each record are listed.

4.2 Arrhythmia Classification Performance

The proposed stochastic SNN architecture, which is made of 20 neurons and has a cyclic topology, was trained to complete a basic nonlinear prediction task. The evaluation duration has been set to $T_{eval}=(2^8-1)\cdot T_{clk}$ and the clock frequency is 1 kHz (T_{clk}=1ms). Figure 17 depicts the register transfer level (RTL) design. The network's performance was assessed for several patient datasets with QRS complex. Figure 18 depicts an example of one patient's ECG classification performance.

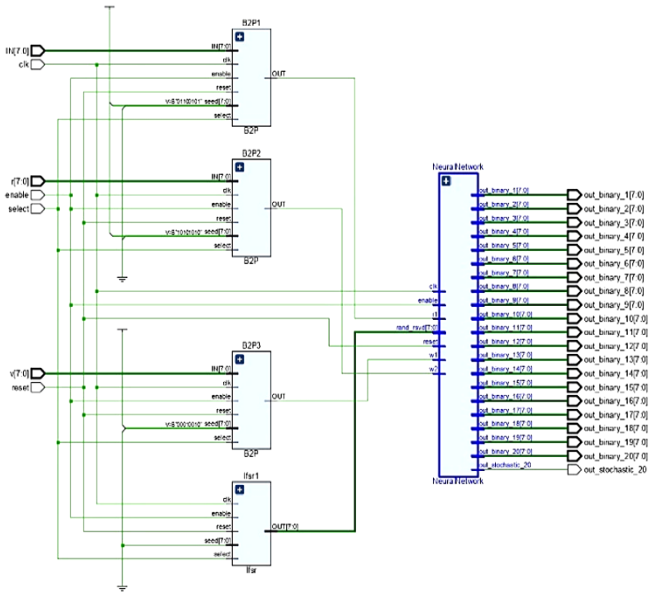

Figure 17. RTL of proposed SNN classifier.

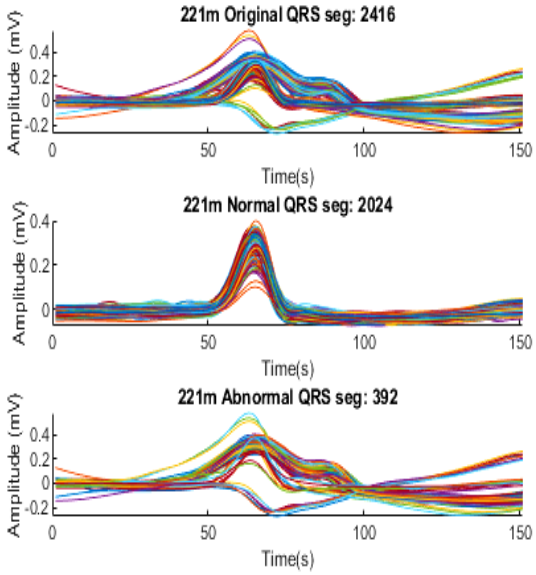

Figure 18. ECG classification performance.

Table 2 shows the confusion matrix for the performance of the proposed ventricular heartbeat classifier. The sensitivity, accuracy and specificity indicators are computed from the confusion matrix using Equations (3), (7) and (8) which are represents as follows.

$$Accuracy = \frac{TP+TN}{TP+FP+FN+TN} \times 100 \quad (7)$$

$$Specificity = \frac{TN}{TN+FP} \times 100 \quad (8)$$

The template matching approach demonstrates that high performance was achieved with sensitivity, accuracy and specificity of 97.41%, 95.10% and 93.68%, respectively. The high accuracy indicates that the system is accurate and efficient in classifying normal and abnormal arrhythmias, while high specificity of abnormal diagnosis indicates the existence of disease with confidence.

Table 2. Confusion matrix of SNN classification.

	True Normal	**True Abnormal**
Prediction Normal	70085	3173
Prediction Abnormal	1862	27578

4.3 Comparison with Previous Study

Previous researchers have worked extensively on reducing the feature size of arrhythmia detection systems. However, they encountered computational burdens. Table 3 highlights the methodologies, feature size and classification performance achieved in the proposed methodology and related studies.

The proposed approach demonstrates that a great performance has been achieved by employing only a single feature as compared to previous research.

Table 3. Comparison with other studies.

The Authors	Method	Feature Size	Accuracy
Venkatesan et al. [14]	kNN	14	97.5%
Ye at al. [15]	SVM	5	86.4%
Vedavathi et al. [16]	kNN	4	98.40%
S. Savalia [17]	MLP; CNN	3	88.7%; 83.5%
S. Nahak et al. [18]	SVM	3	93.33%
Proposed Approach	**SNN**	**1**	**96.91%**

After verifying that the proposed method is effective in classifying heartbeats even with a single-feature size, the proposed system has been implemented in FPGA to demonstrate the hardware efficiency achieved by the minimum feature size used, thus reducing the computational burdens. Table 4 shows the hardware resources needed to implement the proposed SNN ventricular heartbeat classifier synthesized on a Xilinx Zynq-7000 FPGA. The proposed SNN classifier uses the least LUT and FF numbers to accomplish ventricular heartbeat classification, due to the hardware improvements in the MAC designs.

Table 4. Hardware resource utilization comparison.

Reference	[19]	[20]	[21]	**This Approach**
FPGA	Zynq 7000	Spartan 3AN	Zynq 7000	**Zynq 7000**
Classifier type	CoNN	BPNN	MLP	**SNN**
LUT	50284	4321	1963	**692 (0.65%)**
FF	471	3893	1613	**440 (0.83%)**

5. CONCLUSIONS

In this study, a simple and patient-adaptable heartbeat rhythm classification system based on SSNN was developed to obtain the highest performance with the minimum account load. The model only employs QRS complex as the only feature for classification. Moreover, the non-random structure of stochastic neurons connection in reservoir topology makes SSNN models easily implemented in hardware, also resulting in quick processing. The results demonstrate that the detection of QRS complex in MIT-BIH database using Pan-Tompkins and template matching achieves a sensitivity of 99.65%. Meanwhile, the proposed SSNN with correlation coefficient shows high effectiveness in classifying arrhythmia with sensitivity, specificity and accuracy of 99.6%, 98.93% and 96.91%, respectively. Simple processing and hardware resource saving of the architecture in this work provide a substantial contribution to the field of Medical Internet of Things (MIoT).

ACKNOWLEDGEMENTS

The authors acknowledge the technical and financial support by Universiti Teknikal Malaysia Melaka (UTeM) and the Ministry of Higher Education, Malaysia, under the research grant no. FRGS/1/2020/ICT02/UTEM/02/1.

REFERENCES

[1] S. S. Virani et al., "Heart Disease and Stroke Statistics—2021 Update: A Report from the American Heart Association," Circulation, vol. 143, no. 8, pp. e254–e743, 2021.

[2] K. Yasin, "Classification of PVC Beat in ECG Using Basic Temporal Features," Balkan Journal of Electrical and Computer Engineering, vol. 6, no. 2, pp. 78–82, 2018.

[3] F. Zhou, L. Jin and J. Dong, "Premature Ventricular Contraction Detection Combining Deep Neural Networks and Rules Inference," Artificial Intelligence in Medicine, vol. 79, pp. 42–51, 2017.

[4] X. Liu, H. Du, G. Wang, S. Zhou and H. Zhang, "Automatic Diagnosis of Premature Ventricular Contraction Based on Lyapunov Exponents and LVQ Neural Network," Computer Methods and Programs in Biomedicine, vol. 122, no. 1, pp. 47–55, 2015.

[5] M. S. Memon, A. Lakhan, M. A. Mohammed, M. Qabulio, F. Al-Turjman and K. H. Abdulkareem,

"Machine Learning-data Mining Integrated Approach for Premature Ventricular Contraction Prediction," Neural Computing and Applications, vol. 33, no. 18, pp. 11703–11719, 2021.

[6] Y. C. Wong and Y. Q. Lee, "Design and Development of Deep Learning Convolutional Neural Network on an Field Programmable Gate Array," Journal of Telecommunication, Electronic and Computer Engineering, vol. 10, no. 4, pp. 25–29, 2018.

[7] C. Y. Saw, Y. C. Wong, S. L. Loh and H. Zhang, "On-chip Ultra Low Power Optical Wake-up Receiver for Wireless Sensor Nodes Targeting Structural Health Monitoring," Telkomnika, vol. 18, no. 5, pp. 2257–2264, 2020.

[8] Q. Mastoi, T. Ying Wah, R. Gopal Raj and A. Lakhan, "A Novel Cost-efficient Framework for Critical Heartbeat Task Scheduling Using the Internet of Medical Things in a Fog Cloud System," Sensors, vol. 20, no. 2, p. 441, 2020.

[9] F. Corradi et al., "ECG-based Heartbeat Classification in Neuromorphic Hardware," Proc. of the IEEE International Joint Conference on Neural Networks (IJCNN), pp. 1–8, Budapest, Hungary, 2019.

[10] A. F. Murray and A. V. W. Smith, "Asynchronous VLSI Neural Nnetworks Using Pulse-stream Arithmetic," IEEE J. Solid-State Circuits, vol. 23, no. 3, pp. 688–697, 1988.

[11] F. Blayo and P. Hurat, "A VLSI Systolic Array Dedicated to Hopfield Neural Network," Proc. of the VLSI f*or* Artificial Intelligence, Part of the the Kluwer International Series in Engineering and Computer Science Book Series, vol. 68, pp. 255–264, Springer, 1989.

[12] P. Chi et al., "Prime: A Novel Processing-in-memory Architecture for Neural Network Computation in Reram-based Main Memory," ACM SIGARCH Comput. Archit. News, vol. 44, no. 3, pp. 27–39, 2016.

[13] K. Roy, A. Jaiswal and P. Panda, "Towards Spike-based Machine Intelligence with Neuromorphic Computing," Nature, vol. 575, no. 7784, pp. 607–617, 2019.

[14] C. Venkatesan, P. Karthigaikumar and R. Varatharajan, "A Novel LMS Algorithm for ECG Signal Preprocessing and KNN Classifier Based Abnormality Detection," Multimed. Tools Appl., vol. 77, no. 8, pp. 10365–10374, 2018.

[15] C. Ye, B. V. K. V. Kumar and M. T. Coimbra, "Combining General Multi-class and Specific Two-class Classifiers for Improved Customized ECG Heartbeat Classification," Proc. of the 21st IEEE International Conference on Pattern Recognition (ICPR2012), pp. 2428–2431, Tsukuba, Japan, 2012.

[16] V. G. Rangappa, S. Prasad and A. Agarwal, "Classification of Cardiac Arrhythmia Stages Using Hybrid Features Extraction with K-nearest Neighbour Classifier of ECG Signals," Learning, vol. 11, pp. 21–32, 2018.

[17] S. Savalia and V. Emamian, "Cardiac Arrhythmia Classification by Multi-layer Perceptron and Convolution Neural Networks," Bioengineering, vol. 5, no. 2, p. 35, 2018.

[18] S. Nahak and G. Saha, "A Fusion Based Classification of Normal, Arrhythmia and Congestive Heart Failure in ECG," Proc. of the IEEE National Conference on Communications (NCC), pp. 1–6, Kharagpur, India, 2020.

[19] M. Alfaro-Ponce, I. Chairez and R. Etienne-Cummings, "Automatic Detection of Electrocardiographic Arrhythmias by Parallel Continuous Neural Networks Implemented in FPGA," Neural Comput. Appl., vol. 31, no. 2, pp. 363–375, 2019.

[20] M. G. Egila, M. A. El-Moursy, A. E. El-Hennawy, H. A. El-Simary and A. Zaki, "FPGA-based Electrocardiography (ECG) Signal Analysis System Using Least-square Linear Phase Finite Impulse Response (FIR) Filter," J. Electr. Syst. Inf. Technol., vol. 3, no. 3, pp. 513–526, 2016.

[21] M. Wess, P. D. S. Manoj and A. Jantsch, "Neural Network Based ECG Anomaly Detection on FPGA and Trade-off Analysis," Proc. of the IEEE International Symposium on Circuits and Systems (ISCAS), pp. 1–4, Baltimore, MD, USA, 2017.

[22] A. Lakhan et al., "Hybrid Workload Enabled and Secure Healthcare Monitoring Sensing Framework in Distributed Fog-cloud Network," Electronics, vol. 10, no. 16, p. 1974, 2021.

[23] K.-L. Du and M. N. Swamy, "Recurrent Neural Networks," In book: Neural Networks and Statistical Learning, pp. 337–353, 2014.

[24] J. Pan and W. J. Tompkins, "Real-time QRS Detection Algorithm," IEEE Trans. Biomed. Eng., vol. BME-32, no. 3, pp. 230–236, 1985.

[25] Q. Mastoi, T. Y. Wah and R. Gopal Raj, "Reservoir Computing Based Echo State Networks for Ventricular Heart Beat Classification, Applied Sciences, vol. 9, no. 4, p. 702, 2019.

[26] G. M. Friesen, T. C. Jannett, M. A. Jadallah, S. L. Yates, S. R. Quint and H. T. Nagle, "A Comparison of the Noise Sensitivity of Nine QRS Detection Algorithms," IEEE Trans. Biomed. Eng., vol. 37, no. 1, pp. 85–98, 1990.

[27] R. Kher, "Signal Processing Techniques for Removing Noise from ECG Signals," Journal of Biomedical Engineering and Research, vol. 3, pp. 1–9, 2019.

[28] R. VanRullen, R. Guyonneau and S. J. Thorpe, "Spike Times Make Sense," Trends in Neurosciences, vol. 28, no. 1, pp. 1–4, 2005.

[29] M. L. A. Barceló, Methodologies for Hardware Implementation of Reservoir Computing Systems, Ph.D. Thesis, Physics Department, Electronics Engineering Group, Universitat de les Illes Balears, 2017.

[30] T. Y. Wah, R. Gopal Raj et al., "Reservoir Computing Based Echo State Networks for Ventricular Heart Beat Classification," Applied Sciences, vol. 9, no. 4, p. 702, 2019.

[31] H. Jaeger, "Tutorial on Training Recurrent Neural Networks, Covering BPPT, RTRL, EKF and the "Echo State Network" Approach," GMD-Forschungszentrum Informationstechnik Bonn, vol. 5, no. 01, 2002.

[32] F. Ponulak and A. Kasinski, "Introduction to Spiking Neural Networks: Information Processing, Learning and Applications," Acta Neurobiologiae Experimentalis, vol. 71, no. 4, pp. 409–433, 2011.

ملخص البحث:

تُعدّ أمراض القلْب في طليعة أسباب الوفيات على الصّعيد العالمي. ويتطلّب التّصنيف الدّقيق لضربات القلْب عدداً أكبر من السِّمات المستخلَصة، علماً بأنّ ضربات القلب من الصِّنف ذاته يُمكن أن تتصرّف على نحوٍ مختلفٍ من مريض الى آخر. وهذا من شأنه أن يقود الى ارتفاعٍ في تكلفة الحوسبة، إضافةً الى تحدّياتٍ ترتبط بمعدّات الحوسبة المستخدمة، وذلك بالنّظر الى العدد الضّخم من العُقَد في شبكات حوسبة الخزّان (RC).

في هذا البحث، تمّ اقتراح شبكةٍ عصبية ناتئة عشوائية مبنيةٍ على حوسبة الخزّان (SSNN) لتصنيف إيقاعات ضربات القلب، بحيث تسمح باستخدام معدّات حوسبةٍ ملائمة للمرضى بتكلفةِ حوسبةٍ أقلّ بسبب استخدام الحدّ الأدنى من عدد السِّمات المستخلصة. وقد تمّ استخدام سِمَةٍ واحدة فقط لتحقيق ملائمة الشّبكة للمرضى وتقليل تكلفة الحوسبة؛ تلك السِّمة هي مركَّب QRS، وقد جرى استخلاصها وتغذيتها الى الخزّان العصبي بعشْرين عُصبوناً على نحوٍ دوْري من أجل حساب وتصنيف عدم انتظام ضربات القلب. وقد تمّ استخلاص 43 من تسجيلات مخطّط ضربات القلب المحتوية على ضربات قلب طبيعية وأخرى غير طبيعية من قاعدة البيانات الخاصة بعدم انتظام ضربات القلب () التي تمّ الحصول عليها من شبكة (). وقد حقق الخزّان المقترح حساسيةٍ مقدارها 99.6% ودقّة مقدارها 96.91%، الأمر الذي يؤشّر الى أنّ النّظام المقترح دقيق وفعّال في تصنيف حالات عدم انتظام ضربات القلب الطبيعية وغير الطبيعية.